The design and sensitivity of microwave frequency optical heterodyne receivers

S. J. Bingham,[a] B. Börger, and D. Suter
Fachbereich Physik, Universität Dortmund, 44221 Dortmund, Germany

A. J. Thomson
Centre for Metalloprotein Spectroscopy and Biology, School of Chemical Sciences, University of East Anglia, Norwich NR4 7TJ, England

(Received 12 February 1998; accepted for publication 30 June 1998)

Recent advances in high speed photodetector and microwave receiver technology make microwave frequency optical heterodyning an attractive approach for the detection of a number of coherent Raman and Brillouin scattering experiments. We have therefore analyzed the sensitivity of microwave frequency optical heterodyne receivers. Experimental tests on a visible wavelength receiver operating at 13.5 GHz confirm the expectation of shot noise limited sensitivity. The relative merits of microwave frequency optical heterodyne detection and the alternative Fabry–Pérot interferometry approach are discussed. © *1998 American Institute of Physics.* [S0034-6748(98)04309-3]

I. INTRODUCTION

Optical heterodyne detection[1,2] measures an optical signal wave $E\cos\omega t$ by beating it against a second, much more intense ''local oscillator'' wave $E_0\cos\omega_0 t$ at a photodetector. In addition to a large dc current due to the local oscillator the detector produces an oscillating current with a frequency $|\omega-\omega_0|$, and an amplitude proportional to the electrical field strength E of the optical signal. Optical heterodyning is particularly attractive for detecting weak optical signals in the presence of a copropagating laser beam: in the heterodyne experiment, the copropagating beam serves as the local oscillator, but in the case of direct low level detection, it must be suppressed using a narrowband optical filter, such as a Fabry–Pérot interferometer.

It has been possible to perform radio frequency ($\leqslant 1$ GHz) optical heterodyne detection with good sensitivity for many decades. Although a number of ingenious vacuum tube[3,4] and solid state[5,6] detectors that operated at microwave frequencies (1–20 GHz) were demonstrated over 30 years ago, we are only aware of one example of their application in a spectroscopic instrument.[7] This particular device exhibited a very poor quantum efficiency. The same experiment was repeated shortly afterwards with much better sensitivity using direct low level detection in a Fabry–Pérot interferometer based instrument.[8]

In recent years, the requirements of fiber-optic telecommunication have stimulated the development of greatly improved high speed photodetectors.[9] The use of new light absorbing materials and improved fabrication methods has resulted in photodetectors with electrical bandwidths approaching 1 THz.[10–12] Devices with 60 GHz bandwidths and high quantum efficiencies at visible and near infrared wavelengths (400–1700 nm) are now available commercially.[13,14] Of equal importance, since these detectors contain little or no built-in amplification, has been the development of solid state microwave (1–90 GHz) amplifiers with excess noise comparable to or less than room temperature thermal noise.[15,16] The combined application of these technologies allows microwave frequency optical heterodyne detection to be carried out with shot noise limited sensitivity. We have constructed such an instrument and used it to measure 13–14 GHz coherent Raman detected electron paramagnetic resonance of ruby (Cr^{3+}:Al_2O_3)[17] and proteins containing transition metal ions.

The principle aim of this paper is to obtain theoretical expressions relating to the minimum detectable optical signal of a microwave frequency optical heterodyne receiver (Sec. II). The treatment is appropriate to photoreceivers constructed from separate commercial photodetector and amplifier assemblies. In contrast to earlier work[1,3,4,9,18–20] we consider the issues that arise when it is necessary to connect the photodetector and amplifier by a transmission line with a length comparable to or larger than the microwave wavelength. Workers who wish to construct optical heterodyne receivers using microwave integrated circuit techniques will find more appropriate treatments elsewhere.[9,18,19] The calculations allow the sensitivity of practical receivers to be optimized and the feasibility of experiments assessed. In addition, measurements of signal and noise power on our optical heterodyne receiver are presented that demonstrate the practical relevance of these calculations (Sec. III). Finally, the strengths and weaknesses of microwave frequency optical heterodyne detection are compared with Fabry–Pérot interferometry,[21,22] the most likely alternative approach in many applications (Sec. IV).

[a]Electronic mail: Stephen.Bingham@Fuj.Physik.Uni-Dortmund.De

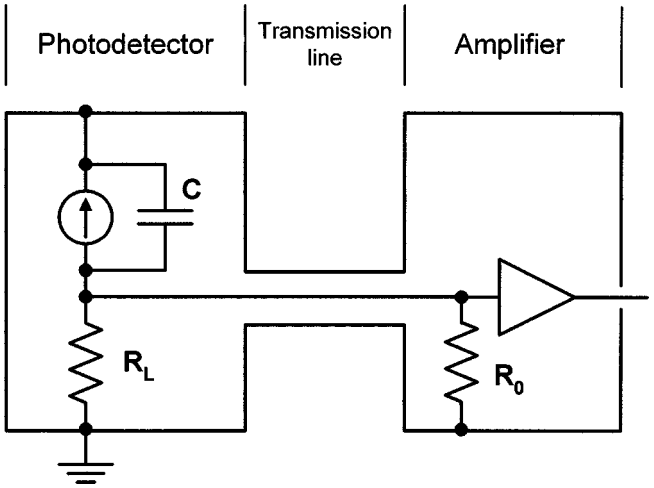

FIG. 1. Simplified photoreceiver electrical schematic, modeling the photodetector element as a current source with associated parasitic capacitance C. The photodetector load resistance R_L and amplifier input impedance R_0 are also shown.

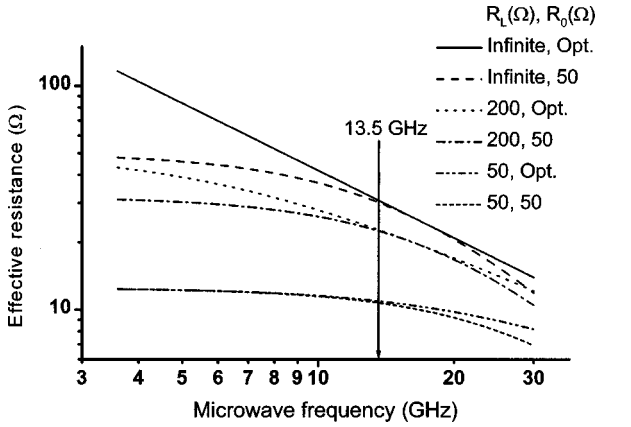

FIG. 2. Effective load resistance R_{eff} as a function of frequency for various load resistances R_L and amplifier input impedances R_0, assuming a parasitic capacitance $C=0.19$ pF.

II. CALCULATION AND OPTIMIZATION OF SENSITIVITY

A. Signal power

Assuming perfect mode overlap between the single frequency optical signal, $E\cos\omega t$, and local oscillator, $E_0\cos\omega_0 t$,[23] the photocurrent is

$$I=\rho(0)(P_0+P_1)+2\rho(\omega_1)\sqrt{P_0P_1}\cos\omega_1 t, \tag{1}$$

where $\rho(0)$ and $\rho(\omega_1)$ are, respectively, the dc and high frequency responsivities (A/W) of the photodetector, $\omega_1=|\omega-\omega_0|$ is the microwave frequency, P_1 is the power of the signal wave, and P_0 is the local oscillator power. The high frequency responsivity $\rho(\omega_1)$ may be less than $\rho(0)$ due to the limited intrinsic speed of the photodetector.

The design and performance of high speed photodetectors has been discussed extensively in the literature.[9,19] In our instrument, we relied on a commercial device, which is packaged with a bias circuit, a load resistor R_L, and a 50 Ω output connector.[13,14] For the following analysis, it is sufficient to model the detector as a current source in parallel with a parasitic capacitance C, as shown in Fig. 1. The signal we wish to observe is proportional to the power $P_{\text{signal}}(\omega_1)$ dissipated by the alternating part of the photocurrent in the input impedance R_0 of the amplifier

$$P_{\text{signal}}(\omega_1)=\frac{2P_0P_1\rho(\omega_1)^2}{R_0[(1/R_L+1/R_0)^2+(\omega_1C)^2]}. \tag{2}$$

For all R_0 the signal power can be increased by increasing the load resistance R_L. On the other hand, the dc photocurrent flowing through the load resistor reduces the bias voltage by an amount proportional to the dc current. In our case, the manufacturers of the photodetector did not recommend a load resistance larger than 200 Ω.[24]

Knowledge of the parasitic capacitance C is essential in modeling both the signal and noise powers. We estimate it from the 3 dB bandwidth ω_C of the photoreceiver circuit. Because of the finite intrinsic speed of the photodetector, the parasitic capacitance is

$$C\leqslant(1/R_L+1/R_0)/\omega_C. \tag{3}$$

For our photodetector package ($R_L=200\ \Omega$, $R_0=50\ \Omega$, $\omega_C=21$ GHz)[25] we obtain $C\leqslant 0.19$ pF.

Using this value of C we can calculate the frequency dependence of the signal power for different values of R_0 and R_L (see Fig. 2). For this purpose it is convenient to introduce an effective load resistance defined by

$$R_{\text{eff}}=\frac{R_0R_L^2}{(R_0+R_L)^2}\frac{1}{1+(\omega_1/\omega_C)^2}. \tag{4}$$

This allows us to write the signal power as

$$P_{\text{signal}}(\omega_1)=2P_0P_1\rho(\omega_1)^2R_{\text{eff}}. \tag{5}$$

For a given photodetector responsitvity $\rho(\omega_1)$, the effective load resistance parametrizes the efficiency of the receiver design. In Fig. 2, we have compared designs as a function of the microwave frequency ω_1. For our instrument, operating at $\omega_1/2\pi=13.5$ GHz, increasing R_L from 50 to 200 Ω increases R_{eff}, and hence the signal power by a factor of 2 (3 dB) when $R_0=50\ \Omega$. An infinite value of R_L would only improve the signal power by a further factor of 1.3 (1 dB). For a given load resistance R_L and parasitic capacitance C, there is an optimum value $R_0(\text{opt})$ of the amplifier input impedance

$$R_0(\text{opt})=\frac{1}{\sqrt{1/R_L^2+(\omega_1C)^2}}. \tag{6}$$

It is possible to change R_0 from the 50 Ω determined by transmission lines and available amplifiers to the optimum value by placing an impedance transforming device between the photodetector and amplifier. The effective resistances obtained with an optimized R_0 are also plotted in Fig. 2. In our case ($\omega_1/2\pi=13.5$ GHz, $C\cong 0.19$ pF, $R_L\cong 200\ \Omega$) no significant improvement can be obtained; the additional losses of an impedance transformer would even degrade the performance.

B. Noise power

In an optical heterodyne detected instrument the microwave frequency signal produced by the photodetector must be amplified and converted to a dc signal using a microwave receiver. The first stage of the microwave receiver is the low noise amplifier considered in the previous section. In a properly designed microwave receiver,[26,27] the other stages do not contribute significant noise to the signal.

Amplifier noise can be modeled by the following contribution to the noise power dissipated in the amplifier input impedance:

$$P_{\text{amplifier noise}} = 290k\Delta\nu(10^{N/10}-1) = kT_E\Delta\nu, \tag{7}$$

where k is Boltzmann's constant, N is the amplifier noise figure in dB, T_E is the equivalent excess noise temperature, and $\Delta\nu$ is the receiver bandwidth. Our instrument employs a 13.5 GHz amplifier with a 1.25 dB noise figure ($T_E = 100$ K). Similar amplifiers operating at cryogenic temperatures generate less noise (e.g., $N=0.48$, $T_E=35$ K, $\omega_1 = 13$ GHz).[15] Cryogenic high electron mobility transistors exhibit noise figures below 0.1 dB ($T_E=7$ K) for frequencies less than 18 GHz.[28] Practical amplifiers employing such devices are expected to show similar performance.

If the amplifier is not attached to a source with a 50 Ω input impedance its noise performance deteriorates. The input impedance of the photodetector assembly is determined by the load resistance R_L and the parasitic capacitance C. Even when R_L is 50 Ω the photodetector is far from 50 Ω resistive at frequencies comparable to ω_C. To avoid deterioration of the receiver noise we insert a ferrite isolator between the photodetector and amplifier. We estimate that this reduces the voltage standing wave ratio[29] in our instrument from 6.9 to less than 1.5 at the expense of 0.25 dB signal attenuation.

The photodetector and isolator radiate thermal noise[1] into the amplifier. The dominant source of thermal noise in the photodetector package is the load resistance R_L. The noise power due to this source dissipated in the amplifier input impedance is

$$P_{\text{load resistance}} = 4kT_L\Delta\nu\frac{R_{\text{eff}}}{R_L}(1-A_I), \tag{8}$$

where T_L is the absolute temperature of the load resistor and A_I is the attenuation due to the isolator. Increasing the load resistance reduces this contribution.

Although an ideal lossless isolator does not radiate thermal noise towards the amplifier, the 50 Ω termination present in the isolator radiates thermal noise towards the photodetector. A transmission line calculation[29,30] shows that the proportion of the isolator noise power reflected by the photodetector is

$$|\Gamma|^2 = 1-4\frac{R_{\text{eff}}}{R_L}, \tag{9}$$

where Γ is the voltage reflection coefficient. Thus the thermal noise power from the isolator termination is

$$P_{\text{isolator termination}} = kT_T\Delta\nu(1-A_I)^2|\Gamma|^2, \tag{10}$$

where T_T is the absolute temperature of the isolator termination and we have assumed that the two passes through the isolator cause the same attenuation.

We should also take into account thermal noise introduced by losses in the isolator. The thermal noise power radiated towards the photodetector and reflected back through the isolator is

$$P_{\text{reflected isolator losses}} = kT_I\Delta\nu(1-A_I)A_I|\Gamma|^2, \tag{11}$$

where T_I is the isolator temperature. Similarly, the thermal noise power radiated towards the amplifier by the losses is

$$P_{\text{forward radiated isolator losses}} = kT_I\Delta\nu A_I. \tag{12}$$

Adding these four contributions shows that for equal photodetector, isolator, and isolator termination temperatures T the total thermal noise power is

$$P_{\text{total thermal noise}} = kT\Delta\nu. \tag{13}$$

This is equal to the thermal noise power radiated backwards by the amplifier. In contrast to low frequency systems it is therefore not possible to reduce thermal noise by simply increasing the load resistance R_L.

It is possible, however, to reduce the thermal noise by cooling either the photodetector load resistance or the isolator termination. In our instrument we estimate that about 50% of the thermal noise power comes from the isolator termination, compared to about 41% from the photodetector load and 9% from the isolator losses. Cooling the isolator termination is a relatively simple matter. This option will be most useful in instruments with low isolator losses and either a larger load resistance, or operating frequencies higher than ω_C, since the isolator termination makes the dominant contribution to thermal noise in these cases. Another option is cooling of the photodetector load. For practical reasons this also implies cooling of the photodetector device. This approach has been demonstrated successfully for a low temperature grown GaAs photoconductor with an electrical bandwidth of $\cong$800 GHz operating at 77 K.[12]

The final noise source we consider quantitatively is shot noise due to the corpuscular nature of photons and charge carriers. For laser light showing the normal Poissonian statistics[31] the mean squared noise current produced by a photodiode is

$$\overline{I_N^2} = 2e\overline{I}\Delta\nu, \tag{14}$$

where e is the electron charge and $\overline{I}$ is the mean photocurrent. In photoconductive detectors, avalanche photodiodes, and photomultiplier tubes additional contributions to the shot noise can be important.[1,9] In an optical heterodyne instrument we may neglect the signal photocurrent $\rho(0)P_1$ relative to that of the local oscillator $\rho(0)P_0$. For a photodiode, the noise power dissipated in the amplifier input impedance is therefore

$$P_{\text{shot noise}} = 2eP_0\rho(0)R_{\text{eff}}(1-A_I)\Delta\nu. \tag{15}$$

In our experiments we use a single mode ring-dye laser as the local oscillator. This source was chosen because of its negligible microwave frequency intensity fluctuations, which can make the dominant noise contribution when other types

of source are used. For example, thermal sources, such as lamps, exhibit intensity fluctuations inherent to their Gaussian statistics.[32] If the optical linewidth Δ is larger than the microwave signal frequency, the mean squared noise current due to this effect is on the order of

$$\overline{I_N^2} \cong \frac{\Delta\nu}{\Delta}\,\overline{I^2}. \tag{16}$$

Even more severe intensity fluctuation noise will arise if a multimode laser serves as the local oscillator[32] and an integer multiple of the mode spacing is close to the microwave signal frequency.

C. Minimum detectable signal

The minimum detectable signal power is usually defined as being equal to the noise power. Allowing for additional losses due to the isolator, the signal power is

$$P_{\text{signal}}(\omega_1) = 2P_0P_1\rho(\omega_1)^2R_{\text{eff}}(1-A_I). \tag{17}$$

From Eqs. (7), (13), and (15) the combined noise power in a photoreceiver employing a photodiode is

$$P_{\text{noise}} = [k(T+T_E) + 2eP_0\rho(0)R_{\text{eff}}(1-A_I)]\Delta\nu. \tag{18}$$

The minimum detectable optical signal power is therefore

$$P_1(\min) = \frac{\dfrac{k(T+T_E)}{2(1-A_I)R_{\text{eff}}} + e\rho(0)P_0}{2\rho(\omega_1)^2P_0\tau}, \tag{19}$$

where τ is the data collection time, which is related to the bandwidth by the relation

$$\Delta\nu = \frac{1}{2\tau}. \tag{20}$$

When shot noise is much larger than other noise sources and $\rho(0) = \rho(\omega_1)$, the minimum detectable signal power reduces to

$$P_1(\min) = \frac{e}{2\rho(0)\tau} = \frac{h\nu}{2\mu\tau}, \tag{21}$$

where μ is the quantum efficiency and ν is the frequency of the optical radiation. Thus, the minimum detectable number of signal photons in a given data collection time is

$$N_{\min} = \frac{1}{2\mu}. \tag{22}$$

In principle, one photon can be detected with a 50% quantum efficiency photodiode.

III. EXPERIMENT

A. Description of the optical heterodyne receiver

A schematic diagram of our optical heterodyne receiver is shown in Fig. 3. The photodetector is a New Focus[13] model 1437 InGaAs Schottky contact photodiode, with a 200 Ω load resistor. The specified wavelength range of the photodiode is 400–1650 nm, with a responsivity of $\rho(0) = 0.2$ A/W ($\lambda = 1060$ nm). The microwave receiver was assembled and tested as a single unit by Miteq.[15] The low noise preamplifier[33] has a specified noise figure of 1.25 and gain between 28.5 and 31.5 dB in the 13.4–14.1 GHz frequency range. The measured attenuation of the isolator[34] is 0.25 dB at 13.5 GHz. The microwave signal is mixed with a tuneable cavity oscillator[35] using a double balanced mixer.[36] The latter has single sideband losses in the range 7.5–10 dB depending on local oscillator and intermediate frequency. Two low frequency amplifiers are used to further amplify the signal. The combined gain of these amplifiers is 64.4 dB at 50 kHz, the frequency of a secondary modulation system typically used in our instrument.[17]

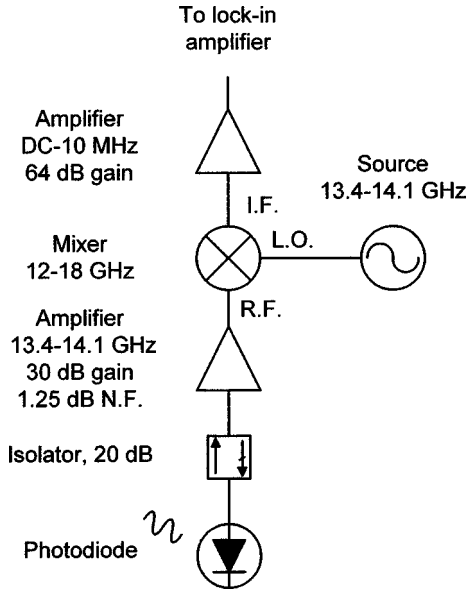

FIG. 3. Schematic diagram of the optical heterodyne receiver used in our experiments. Further details of the most important components are given in the text.

B. Noise power tests

Noise measurements were made with a lock-in amplifier[37] with its reference frequency set to 50 kHz and a time constant of 300 ms. With no laser radiation incident on the detector a root-mean-square (rms) noise voltage of 13–14 $\mu V/\sqrt{\text{Hz}}$ was observed in each phase channel across the 50 Ω termination of the fully assembled optical heterodyne receiver, including low frequency amplifiers. When a 50 Ω termination is placed on the input of the low frequency amplifiers an rms noise voltage of 1.2 ± 0.2 $\mu V/\sqrt{\text{Hz}}$ is observed under the same conditions, confirming the negligible contribution made by these amplifiers. Further measurements were made with laser powers of up to 9 mW incident on the photodetector. The observed dependence of the noise power on the photocurrent is shown in Fig. 4. From Eq. (18) we expect that the combined thermal, amplifier, and shot noise in our instrument is

$$P_{\text{noise}}/\Delta\nu = 2[k(T+T_E) + 2e\overline{I}R_{\text{eff}}(1-A_I)]G, \tag{23}$$

where G is the combined gain of the microwave amplifier, mixer, and low frequency amplifiers. The additional factor of 2 compared with previous equations arises from our use of a

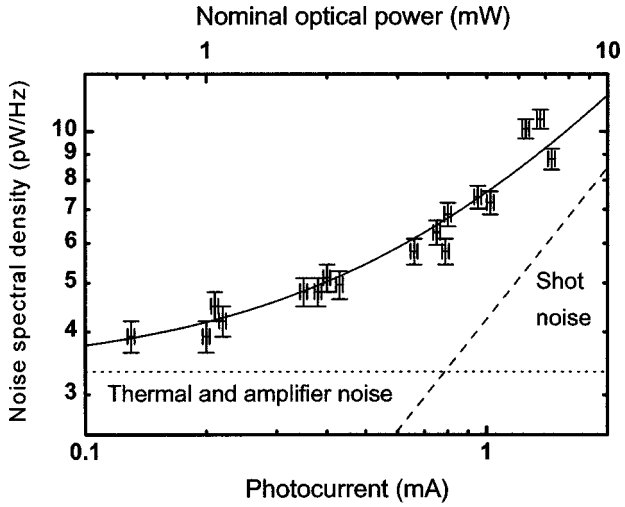

FIG. 4. Measured noise spectral density at the output of the low frequency amplifiers as a function of the dc photocurrent. An equivalent optical power scale calculated for a nominal responsivity $\rho(0)$ of 0.2 A/W is also shown. Also plotted is the theoretical noise power calculated using Eq. (24).

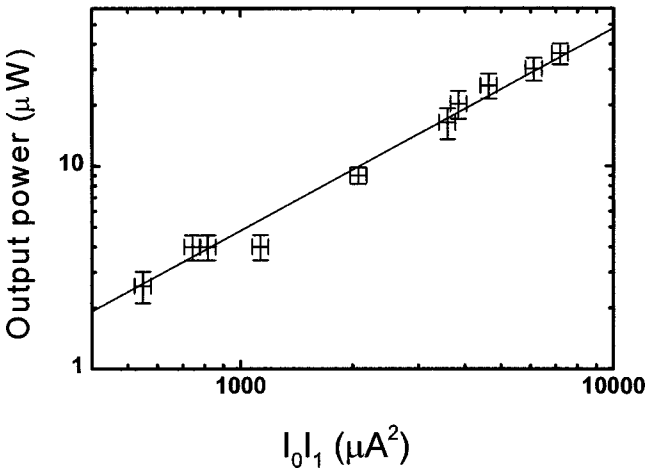

FIG. 5. Signal power produced at the output of the microwave mixer as a function of the product of the dc photocurrents due to the optical local oscillator and signal I_0I_1 in a two laser heterodyning test described in the text. Also shown is the theoretical signal power.

double balanced mixer, which passes noise both above and below the microwave local oscillator frequency.[38] When evaluated using parameters appropriate to our instrument [$T=300$ K, $T_E=100$ K, $R_0=50\ \Omega$, $R_L=200\ \Omega$, $A_I=0.056$ (0.25 dB loss), $\omega_1/2\pi=13.5$ GHz, $\omega_C/2\pi=21$ GHz, G $=3.1\times10^8$ (84.9 dB)], this expression is in excellent agreement with the experimental data. Figure 4 compares the theoretical noise power (solid line) with the experimental data (crosses) and indicates the contributions of shot and photocurrent independent noise (dashed lines). For local oscillator powers greater than about 4 mW, shot noise makes the dominant contribution.

C. Signal power tests

To verify the expression for the signal power obtained above, we heterodyned two single mode ring-dye lasers[39] operating at 597 nm. The more intense laser acted as the local oscillator, the weaker imitated the optical signal. To ensure interference between the two lasers, they were combined in a single mode optical fiber and then passed through a polarizer. The power from each laser incident on the photodiode was measured with an optical power meter.[40] The frequency of the microwave local oscillator was set to 13.5 GHz and the difference between the two laser frequencies was adjusted to approximately the same value using a high resolution wavelength meter.[41] The beat signal between the microwave optical heterodyne signal and the microwave local oscillator was displayed on an oscilloscope.[42] Due to its relatively high level, the signal was sampled directly after the microwave mixer rather than after the low frequency amplifiers which would have become saturated. Measurements were performed at beat frequencies of a few MHz, a value determined by the short term relative frequency jitter of the lasers.

Beat signals were measured for optical local oscillator powers from 640 μW to 7 mW and optical signal powers between 12.5 and 290 μW. The dc responsivity $\rho(0)$ was measured for each data point. Values between 0.15 and 0.23 A/W were obtained. The variation can be accounted for by differences in focusing and optical alignment. Figure 5 shows the measured signal power plotted against the product of the dc photocurrents due to the optical local oscillator I_0 and signal I_1. From Eq. (5) we expect the signal power to be

$$P_{\text{signal}}(\omega_1)=2R_{\text{eff}}\frac{\rho(\omega_1)^2}{\rho(0)^2}(1-A_I)G_{\text{frontend}}I_0I_1, \qquad (24)$$

where G_{frontend} is the combined gain of the microwave amplifier and mixer. From the value of G used to simulate the noise measurements and the gain callibration of the low frequency amplifiers (64.4 dB), we expect that G_{frontend} is close to 112 (20.5 dB) for an intermediate frequency of 50 kHz. It is reasonable to assume that mixer losses, and hence G_{frontend}, at a few MHz intermediate frequency are close to those at 50 kHz. Combining this estimate of G_{frontend} with the other parameters appropriate to our instrument and assuming that $\rho(\omega_1)=\rho(0)$, we find that Eq. (24) is in excellent agreement with the experimental data, as shown in Fig. 5. There is no evidence, within the uncertainty of the data, for optical or microwave power saturation effects.

By inserting the parameters used to simulate the signal and noise power tests into Eq. (24) we can estimate the minimum detectable signal power in a real experiment. For a local oscillator power of 1 mW we find a minimum detectable optical signal power of 2×10^{-18} W in a data collection time of 1 s, equivalent to six 600 nm optical photons. Increasing the local oscillator power to its maximum specified value (10 mW) would reduce the minimum number of detectable photons to 1.7. This performance is equivalent to that of an ideal low level detector with a 60% quantum efficiency.

IV. COMPARISON WITH FABRY–PÉROT INTERFEROMETRY

When considering whether it is appropriate to use microwave frequency optical heterodyne detection in a specific experiment it is usually necessary to compare the method with Fabry–Pérot interferometry. In this section we address

some of the issues relevant to such a comparison. Fabry–Pérot instruments are widely employed in Brillouin and Raman spectroscopy.[8,21,22,43–47]

A. Temporal coherence

Our expressions for signal power and hence for sensitivity are only valid for a linear optical heterodyne receiver, i.e., one in which the electrical signal power is proportional to the optical signal power. Furthermore, we assume that all the electrical signal power is confined in a spectral region small compared to the detection bandwidth $\Delta\nu$. Since the natural linewidths of spectroscopic transitions and optical sources are always much larger than $\Delta\nu$ (typically $\cong 1$ Hz), our treatment is limited to coherent spectroscopic experiments. An example of such an experiment is coherent Raman detected electron paramagnetic resonance,[17] where the frequency of the optical signal is the sum or difference of the optical and microwave excitation frequencies. By mixing the optical signal with the laser and microwave oscillators used to excite the sample the frequency fluctuations in both sources are normally removed from the signal. This also allows the phase relationship between the optical signal and the exciting fields to be studied and hence signals analogous to the magnetic resonance absorption and dispersion to be obtained.[17] Such phase information cannot be obtained with a Fabry–Pérot instrument.

The use of a square-law detector to measure the electrical signal power allows optical heterodyne detection to be employed when the temporal coherence required by linear receivers is not present. However, the sensitivity of square-law optical heterodyne receivers is always poor in absolute terms. Fabry–Pérot instruments, or other instruments employing low level detection, will almost always show better sensitivity. The motivation for using square-law optical heterodyne detection is the arbitrarily high *resolution* that can be obtained,[32] particularly when mixing with the exciting laser removes its contribution to the linewidth. In contrast, the Fabry–Pérot technique is limited in practice to resolutions of about 1 MHz.

B. Light gathering power

Optical heterodyne receivers employing a spatially coherent (laser) local oscillator have a solid angle field of view Ω_H (steradians) and entrance aperture A_H related to each other by the simple relationship: $A_H\Omega_H \cong \lambda^2$, where λ is the optical wavelength.[23] The solid angle field of view Ω_{FP} of a Fabry–Pérot interferometer is of the order of λ/QS, where S is the plate separation and Q is the resonator quality factor. For visible wavelengths, separations appropriate to a microwave frequency free spectral range and $Q \cong 10^4$, Ω_{FP} is on the order of 10^{-8}. Importantly, the area A_{FP} of the entrance aperture is not dependent on Ω_{FP}, so no fundamental limit to the light gathering power exists. However, A_{FP} is typically on the order of 10^{-4} m^2, giving $\Omega_{\mathrm{FP}}A_{\mathrm{FP}} \cong 10^{-12}$ m^2 compared to $\Omega_H A_H \cong 3\times 10^{-13}$ m^2 for a visible optical heterodyne receiver. Thus, the light gathering power of both methods is comparably poor and both experience difficulties when detecting spatially incoherent radiation such as that from scattering experiments or luminescence.

C. Background radiation

An important property of linear optical heterodyne receivers is their very low sensitivity to background radiation. Since the heterodyne receiver is a very narrow bandpass instrument, with an effective width determined by the detection bandwidth $\Delta\nu$, it rejects all background radiation outside of this range. Luminescence, for example, is suppressed by a factor on the order of the optical linewidth (at least 10^9 Hz in solids) divided by $\Delta\nu$ (typically less than 1 Hz). In a Fabry–Pérot interferometer, the suppression of broadband background is given by the resonator quality factor Q (typically 10^3 or 10^4).

For narrowband background radiation, such as scattered or transmitted laser light, the rejection ratio of the Fabry–Pérot instrument is limited by its contrast, which is on the order of 10^4 for a single pass instrument. It is therefore often necessary to pass the light through several interferometers or, more conveniently, several times through a single interferometer. Triple and quintuple pass systems with contrasts better than 10^9 have been employed in Brillouin scattering experiments.[21] When co-propagating transmitted laser excitation is present, as is the case in coherent Raman detected magnetic resonance, even such a suppression ratio limits the applicability of the Fabry–Pérot technique to relatively intense Raman fields. For example, according to the measurements reported here, our heterodyne instrument can detect six Raman photons in the presence of 1 mW of 597 nm laser radiation for a 1 s data collection time. A hypothetical Fabry–Pérot instrument with 100% quantum efficiency and no noise sources other than the shot noise due to the arrival of photons at the detector must have a contrast in excess of 10^{14} in order to show similar performance. As the quantum efficiency, including the Fabry–Pérot transmission, decreases even higher contrasts are required. If the quantum efficiency falls below 17% then the heterodyne instrument will be superior irrespective of the interferometer contrast. There are considerable practical difficulties in achieving such high contrasts while simultaneously maintaining high optical throughput and preventing other noise sources from making a dominant contribution. Obtaining a photon counting detector with a 17% quantum efficiency and sufficiently low dark current is also a severe problem. For example, S-20 photomultiplier tubes have a quantum efficiency of about 10% at 597 nm.[1] Although solid state detectors such as avalanche photodiodes have better quantum efficiencies, their dark currents are too high even when operated at cryogenic temperatures.[48]

Unfortunately, quantitative measurements of the sensitivity of operating Fabry–Pérot instruments are very rare in the literature. A microwave frequency coherent Raman detected electron paramagnetic resonance experiment[44] prior to our own work[17] used a combination of polarization selection and a single pass Fabry–Pérot interferometer to detect Raman signals five orders of magnitude smaller than the laser power. Using a triple pass interferometer and crossed polarizers, signals in coherent Raman detected ferromagnetic[46]

and antiferromagnetic[47] resonance experiments six or seven orders of magnitude smaller than the transmitted laser were detected with a good signal to noise ratio.

V. DISCUSSION

The sensitivity of a practical microwave frequency optical heterodyne receiver has been analyzed. Signal and noise power measurements are in good agreement with the theoretically derived expressions. Shot noise limited sensitivity has been demonstrated experimentally.

Microwave frequency optical heterodyne detection will be most useful in ''coherent'' experiments where optical and microwave local oscillators are available with a fixed phase relationship to that of the signal. The extremely high immunity of optical heterodyne detection to background radiation means that shot noise limited performance can be achieved in all but the most extreme cases provided that sufficient optical local oscillator power is available. The high quantum efficiency of modern microwave frequency photodetectors means that the absolute sensitivity better than practical photon counting instruments will normally be obtained in the visible and near infrared (400–1700 nm).

Optical heterodyne detection is particularly well suited to the measurement of coherent Raman detected electron paramagnetic resonance.[17] In these experiments the transmitted laser beam is a convenient local oscillator since it copropagates with the signal wave. Like the conventional electron paramagnetic resonance experiment,[49] the best resolved spectra should be obtained at microwave (1–300 GHz) frequencies for almost all materials. Until now, the wide application of the coherent Raman detected electron paramagnetic resonance has been hampered by the lack of a sufficiently sensitive instrument operating at these frequencies. Microwave frequency optical heterodyne detection is likely to be useful in similar spectroscopic methods, such as coherent Brillouin scattering[21,22] and coherent Raman detection of hyperfine splittings.[7,8]

ACKNOWLEDGMENTS

This work would not have been possible without the assistance of Arthur Schweiger, Jörg Forrer (ETH, Zürich, CH), Tony Strike (Chemical Sciences, UEA, Norwich, UK), and Bill Roehrich (Miteq, Hauppauge, New York). Financial support was provided by the Royal Society, the Deutsche Forschungsgemeinschaft, and the Graduiertenkolleg Festkörperspektroskopie.

[1] A. Yariv, *Optical Electronics* (Saunders, Philadelphia, PA, 1991).
[2] A. T. Forrester, J. Opt. Soc. Am. **51**, 253 (1961).
[3] L. K. Anderson and B. J. McMurtry, Appl. Opt. **5**, 1573 (1966).
[4] A. E. Siegman, S. E. Harris, and B. J. McMurtry, *Symposium on Optical Masers*, edited by J. Fox (Wiley, New York, 1963), p. 551.
[5] R. P. Riesz, Rev. Sci. Instrum. **33**, 994 (1962).
[6] L. K. Anderson, *Symposium on Optical Masers*, edited by J. Fox (Wiley, New York, 1963), p. 549.
[7] B. S. Mathur, H. Tang, R. Bulos, and W. Happer, Phys. Rev. Lett. **21**, 1035 (1968).
[8] H. Tang and W. Happer, Phys. Rev. Lett. **24**, 551 (1970).
[9] D. Wood, *Optoelectronic Semiconductor Devices* (Prentice Hall, New York, 1994).
[10] Y. Chen, S. Williamson, T. Brock, F. W. Smith, and A. R. Calawa, Appl. Phys. Lett. **59**, 1984 (1991).
[11] S. Y. Chou, Y. Liu, and P. B. Fischer, Appl. Phys. Lett. **61**, 477 (1992).
[12] S. Verghese, K. A. McIntosh, and E. R. Brown, IEEE Trans. Microwave Theory Tech. **45**, 1301 (1997).
[13] NewFocus, Inc., 2630 Walsh Avenue, Santa Clara, CA 95051; http://www.newfocus.com, Contact@NewFocus.com
[14] Newport, Inc., 1791 Deere Ave., Irvine, CA 92714.
[15] Miteq, 100 Davids Drive, Hauppauge, NY 11788; http://www.miteq.com
[16] D.-W. Tu, S. W. Duncan, A. Eskandarian, B. Golja, B. C. Kane, S. P. Svensson, S. Weinreb, and N. E. Byer, IEEE Trans. Microwave Theory Tech. **42**, 2590 (1994).
[17] S. J. Bingham, D. Suter, A. Schweiger, and A. J. Thomson, Chem. Phys. Lett. **266**, 543 (1997).
[18] G. P. Vello-Coleiro, IEEE Electron Device Lett. **9**, 269 (1988).
[19] E. John and M. B. Das, IEEE Trans. Electron Devices **41**, 162 (1994).
[20] S. R. Forrest, J. Lightwave Technol. **3**, 347 (1985).
[21] J. R. Sandercock, Top. Appl. Phys. **51**, 173 (1982).
[22] A. S. Borovik-Romanov and N. M. Kreines, Phys. Rep. **81**, 351 (1982).
[23] A. E. Siegman, Appl. Opt. **5**, 1588 (1966).
[24] R. Marsland, New Focus Inc. (personal communication).
[25] New Focus' callibration ($\lambda = 1060$ nm, 0.9 mW power).
[26] T. H. Wilmshurst, *Electron Spin Resonance Spectrometers* (Adam Hilger, London, 1967).
[27] C. P. Poole, *Electron Spin Resonance: A Comprehensive Treatise on Experimental Techniques* (Wiley, New York, 1983).
[28] J. A. Fendrich and M. Feng, Appl. Phys. Lett. **72**, 368 (1998).
[29] S. Y. Liao, *Microwave Circuit Analysis and Amplifier Design* (Prentice–Hall, Englewood Cliffs, NJ, 1987).
[30] *Microwave Engineers' Handbook*, edited by T. S. Saad (Artech House, Dedham, 1971).
[31] R. Loudon, *The Quantum Theory of Light*, 2nd ed. (Oxford University Press, Oxford, 1983).
[32] H. Z. Cummins and H. L. Swinney, Prog. Opt. **8**, 133 (1970).
[33] Miteq, Amplifier, Model AMF-4F-134141-12.
[34] Harriss, Isolator, Model S130160.FFT.
[35] Miteq, Cavity oscillator, Model OTC-1CM-134141-15P-AFC.
[36] Miteq, Double balanced mixer, Model MDZ0172.
[37] Stanford Research Instruments, Lock-in amplifier, Model SR-830.
[38] This effect can be suppressed by using an image rejection mixer. However, the use of such a mixer in our instrument would degrade the sensitivity due to the presence of modulation sidebands both above and below the microwave local oscillator frequency.
[39] Coherent, Ring-Dye laser, Model 899-21.
[40] Metrologic, Optical power meter, Model 45-545.
[41] Atos, Wavelength meter, Model LM-007.
[42] Hewlett Packard, Digital oscilloscope, Model 54520A.
[43] W. J. Brya, S. Geschwind, and G. E. Devlin, Phys. Rev. **6**, 1924 (1968).
[44] R. Romestain, S. Geschwind, G. E. Devlin, and P. A. Wolff, Phys. Rev. Lett. **33**, 10 (1974).
[45] W. D. Wilber, W. Wettling, P. Kabos, C. E. Patton, and W. Jantz, J. Appl. Phys. **55**, 2533 (1984).
[46] A. S. Borovik-Romanov, V. G. Zhotikov, N. M. Kreines, R. Laiho, and T. Levola, J. Phys. C **13**, 879 (1980).
[47] A. S. Borovik-Romanov, V. G. Zhotikov, N. M. Kreines, and A. A. Pankov, JETP Lett. **23**, 649 (1976).
[48] N. G. Woodard, E. G. Hufstedler, and G. P. Lafyatis, Appl. Phys. Lett. **64**, 1177 (1994).
[49] A. Abragam, and B. Bleaney, *Electron Paramagnetic Resonance of Transition Ions* (Oxford University Press, Oxford, 1970).